Low Temperature Physics/Fizika Nizkikh Temperatur, 2017, v. 43, No. 10, pp. 1471–1481

How does the break-junction quasiparticle tunnel conductance look like for *d*-wave superconductors?

Alexander M. Gabovich and Alexander I. Voitenko

Institute of Physics, National Academy of Sciences of Ukraine, 46 Nauki Ave., Kyiv 03680, Ukraine
E-mail: gabovich@iop.kiev.ua, voitenko@iop.kiev.ua

Received February 28, 2017, published online August 27, 2017

The bias-voltage, V, dependences of the differential tunnel conductance $G(V) = dJ/DV$ were calculated for the quasiparticle current J flowing in the *ab* plane across the break junction made of *d*-wave superconductors. The tunnel directionality effect was taken into account by introducing an effective tunneling cone described by the angle $2\theta_0$. It was shown that $G(V)$ looks like predominantly *d*-wave or isotropic *s*-wave ones, depending on the magnitude of θ_0 and the rotation angles of the crystal lattices of electrodes with respect to the junction plane. In certain configurations, the $G(V)$ dependences of nominally symmetric S–I–S junctions may turn out similar to those for non-symmetric S–I–N junctions (here, S, I, and N denote superconductors, insulators, and normal metals, respectively) and provide misleading information about the actual energy gap. At finite temperatures, subgap structures appear, which possess features appropriate to both *d*- and *s*-wave superconductors and are dependent on the problem parameters.

PACS: 74.20.Rp Pairing symmetries (other than *s*-wave);
74.55.+v Tunneling phenomena: single particle tunneling and STM;
74.72.–h Cuprate superconductors.

Keywords: *d*-wave superconductivity, quasiparticle tunnel conductivity, tunnel directionality, break junctions, high-T_c superconductors.

1. Introduction

Although high-T_c cuprate superconductors were discovered more than three decades ago [1,2], two major problems in their physics still remain unresolved. These are the mechanism of Cooper pairing, i.e., the nature of mediating boson [3–8], and the superconducting order parameter symmetry [9,10]. The both issues are interlinked to a certain extent [11,12]. One should bear in mind that, in principle, superconductivity in high-T_c oxides might be induced by bipolaron condensation [13] or another, even more exotic phenomenon [14]. Nevertheless, the whole body of experimental data testifies that the old good Bardeen–Cooper–Schrieffer (BCS) scenario of superconductivity [15,16] is valid for those materials if the corresponding strong-coupling modifications are made [8,17]. Therefore, in this work, we will restrict the interpretation of superconductivity in oxides to the BCS scheme, whatever the specific pairing mechanism.

Nevertheless, even if the BCS picture is taken for granted, the gluing agent cannot be unambiguously elucidated. Indeed, phonons always exist in solids, whereas spin fluctuations, which are revealed in direct experiments for cuprate samples in certain oxygen doping ranges [18–26], might be relevant to superconductivity or not, but the conclusion cannot be made solely on the basis of their persistence. On the other hand, the order parameter symmetry can be checked directly in phase-sensitive studies dealing with the Josephson tunnel current [10,27–35]. The vast majority of the scientists working in this field think that the *d*-wave symmetry of the superconducting order parameter in cuprates has been unambiguously proved by the experiments indicated above. However, there are other, although less numerous, phase-sensitive measurements, which testify that the *s*-wave (isotropic) contribution to the overall order parameter can be at least very significant [9,35–42]. Hence, the problem still remains to be solved.

At the same time, quasiparticle tunnel measurements can also probe the pairing symmetry, although indirectly. It is so, because the form of the resulting dependences of the junction tunnel conductance G on the bias voltage V applied across the tunnel junction ($G(V)$, the conductance-voltage characteristic, CVC) is associated with the structure of the superconducting order parameter in the momentum space. In particular, since the isotropic *s*-wave super-

conductor (S_i) has no gap nodes on its Fermi surface (FS), the zero-temperature ($T = 0$) conductance equals zero ($G = 0$) in the zero-voltage vicinity $|V| < \Delta$ for the S_i–insulator–normal metal (S_i–I–N) junction and $|V| < \Delta + \Delta'$ for the S_i–I–S_i' ones [43–45], where Δ and Δ' are the gaps in the corresponding s-wave electrodes. Tunnel junctions involving the conventional weak-coupling isotropic superconductors, e.g., tin or aluminum, reproduce the behavior of quasiparticle current theoretically predicted pretty well making no allowance for the directional tunneling [46–48], because this phenomenon does not reveal itself for isotropic superconductors.

On the other hand, since the d-wave superconductor (S) has a cosine-like order parameter in the momentum space ($\Delta(\theta) \propto \cos 2\theta$; hereafter, the angle θ is reckoned from the $\mathbf{k}_x$-axis direction) and thus includes nodes ($\Delta = 0$) on the FS, the zero-temperature CVCs for tunnel junctions including d-wave electrodes are supposed to be quite different. In particular [49,50] (see Fig. 1), the dependence $G(V)$ has a V-shape form near the bias-voltage origin $V = 0$ for the S–I–N junctions (panel a), and an U-like form for the S–I–S ones (panel b). We emphasize that the demonstrated CVC profiles [49,50], as well as the CVCs calculated in the framework of the modified Won–Maki approach [51], were obtained both assuming the noncoherent quasiparticle tunneling through the junction and neglecting the tunnel directionality. This issue will be discussed below.

The quasiparticle current in structures involving layered cuprates may be directed perpendicularly to the layers, i.e. along the crystal c axis. Such a situation is realized, e.g., in mesas [52–57]. In this case, tunneling is predominantly incoherent [9], and it was considered by us earlier [58–61] with the special emphasis on the possible influence of the charge density wave (CDW) manifestations. It might also happen, that in the specific case of $Bi_2Sr_2CaCu_2O_{8+\delta}$, the incoherent tunneling along the c axis, which is inherent to underdoped oxide compositions, becomes coherent for overdoped ones due to the "metallization" of the Bi–O layers [56].

There is, however, another effective method to probe the gapped energy spectrum of superconductors, namely the break-junction technique [62–70]. It should be noted that break junctions are most often fabricated from single crystals in such a manner that the measured Josephson or quasiparticle tunnel currents should flow along the CuO_2 planes [71–73]. However, the crystals can be easily cleaved along the ab planes during the junction fabrication, and there is a large probability that a configuration is formed in which tunneling occurs along the c axis [74]. Break junctions with high-T_c oxides can also be intentionally produced to ensure tunneling along the c axis with clear-cut gap-edge features [75]. Actually, quasiparticle current conductances of break junction samples, descending from the same crystal batch, can demonstrate a certain variety of different tunnel directions with respect to the crystal axes and some kind of gap-averaging in the lateral junction plane [63]. It seems reasonable that broken polycrystalline samples should exhibit a mixture of c-axis and in-plane properties of $G(V)$ with peculiarities located at the same gap positions, as was shown, e.g., for $Bi_2Sr_2CaCu_2O_{8+\delta}$ [75].

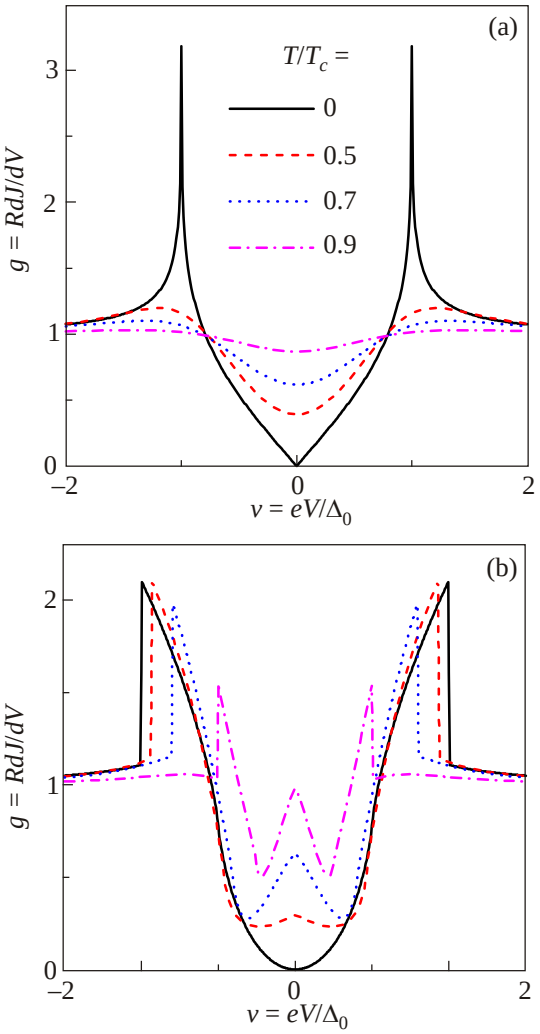

Fig. 1. (Color online) Dimensionless conductance-voltage characteristics (CVCs) $g(v)$ for the quasiparticle current J through nonsymmetric (S–I–N, panel (a)) and symmetric (S–I–S, panel (b)) tunnel junctions with d-wave superconductors at various reduced temperatures T/T_c making no allowance for the directionality (the Won–Maki model [49]). S, I, and N mean d-wave superconductors, insulators, and normal metals, respectively; $g = R\,dJ/dV$; $v = eV/\Delta_0$; R is the normal-state junction resistance; V is the bias voltage; Δ_0 is the superconducting order parameter amplitude at $T = 0$; T_c is the critical temperature.

In this article, we calculate the tunnel conductance for break junctions between d-wave superconductors. This formulation allows us to describe not only cuprates but also other layered superconductors [42], where such an order parameter symmetry is realized. To reduce the number of problem parameters, we leave complications connected with the possible c axis tunnel current leakage beyond the

scope of consideration and analyze the coherent break-junction quasiparticle tunneling directed strictly along the *ab* plane. At the same time, the two broken pieces (the junction electrodes) of the original *d*-wave superconducting sample can be arbitrarily rotated (in this plane) with respect to the junction face. The theoretical picture is intentionally somewhat idealized to trace only the gross features of the superconductivity itself; in particular, without the inevitable (for high-T_c oxides) CDWs [26,60,76–78], although the additional energy gaps induced by the latter are well known to severely distort the actual conductance $G(V)$ dependences of high-T_c oxides [58–61].

The quasiparticle tunneling is assumed coherent (see below), because the coherent Josephson currents are usually observed in such geometrical configurations [79–81]. In the coherent tunneling approximation, the directionality effects [82–86] are very important. They are treated here in the phenomenological manner, because the details are not crucial. The results obtained show how possible electrode rotations, when combined with the tunnel directionality, can drastically change the $G(V)$ patterns in break-junction experiments. For instance, the behavior of $G(V)$ for the intrinsically *d*-wave superconductors can resemble that for the isotropic *s*-wave ones. We show also that sometimes the nominally S–I–S configuration, with break junctions being a subset, may demonstrate an apparent S–I–N behavior. Finally, we attract attention to the insensitivity of the quasiparticle tunnel current to the phase of the anisotropic order parameter. Therefore, contrary to the case of the Josephson current [28,31,79–81,87–91], our results completely coincide with those for the so-called extended *s*-wave superconducting order parameter [92–97] proportional to $|\cos 2\theta|$ in the **k** space.

2. Formulation of the problem

We consider the quasiparticle tunneling in the *ab* plane between two pieces of a layered $d_{x^2-y^2}$-superconductor formed as a result of break-junction fabrication [62–70]. The phenomenological tunnel-Hamiltonian approach is used [44,98]. As was indicated above, we assume the coherent character of tunneling, i.e., when a quasiparticle preserves its momentum (and spin projection) while passing through the junction barrier. Bearing in mind the electron structure of high-T_c oxides, we confine the consideration to the strictly two-dimensional case (see Fig. 2), i.e. we neglect possible current deviations into *c*-axis-directed trajectories [74]. Then, the expression for the tunnel current between the unbiased (0-) and *V*-biased (V-) electrodes looks like

$$J(V) \sim \int_{-\pi/2}^{\pi/2} d\theta \cos\theta \int_{-\infty}^{\infty} d\omega\, Y(\omega,\theta) \times$$

$$\times K(\omega,V,T) N(\omega,\theta) N'(\omega - eV,\theta), \qquad (1)$$

where e is the elementary charge, and the other notations are as follows.

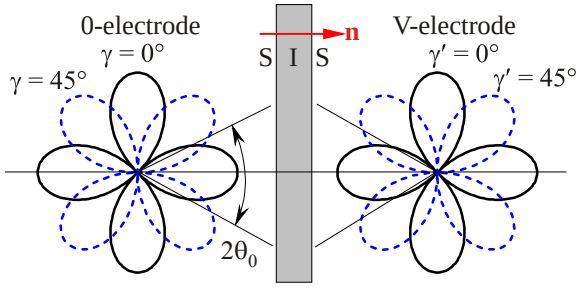

Fig. 2. (Color online) Schematic diagram illustrating the tunnel break-junction configuration and its main parameters: γ and γ' are the rotation angles of the 0- and V-electrodes with respect to the normal **n** to the junction plane, and $2\theta_0$ is the directionality cone. See further explanations in the text.

The unprimed and primed variables correspond to the 0- and V-electrodes, respectively (Fig. 2). The integration variable θ is the angle in the *ab* plane at which the quasiparticle crosses the junction (the angle between the quasiparticle momentum and the normal vector to the junction, **n**). The integration interval $[-\pi/2, \pi/2]$ for θ means that only quasiparticles in the 0-electrode with "positively directed" projections of their momenta on the normal to the junction give a contribution to the total current. The inverse current through the barrier, taken into account by Eq. (1) along with the direct-current counterpart, is provided by quasiparticles in the V-electrode with "negatively directed" projections of their momenta on the normal to the junction. However, since the order parameters in both electrodes are symmetric with respect to their rotation by an angle of π, the integration interval over the angle θ' within the interval $[\pi/2, 3\pi/2]$ is equivalent to the integration over the interval $[-\pi/2, \pi/2]$. The functions $N(\omega,\theta)$ and $N'(\omega - eV,\theta)$ are the partial quasiparticle densities of states in the 0- and V-electrodes, respectively. The energy variable ω is reckoned from the 0-Fermi level, and, in the anisotropic BCS approximation,

$$N(\omega,\theta) = N_F \operatorname{Re} \frac{|\omega|}{\sqrt{\omega^2 - \Delta^2(T,\theta)}}, \qquad (2)$$

where N_F is the normal-state electron density of states at the Fermi level. The function $\Delta(T,\theta)$ is the *d*-wave (or extended *s*-wave) superconducting gap profile in the momentum space at the temperature T (the Boltzmann constant $k_B = 1$).

The coherent character of tunneling means that the transition takes place only between those quasiparticle states on both sides of the barrier that are characterized by the same angle θ. The appearance of the Fermi-distribution-driven function

$$K(\omega,V,T) = \tanh\frac{\omega}{2T} - \tanh\frac{\omega - eV}{2T} \qquad (3)$$

is associated with the temperature-dependent evolution of the quasiparticle states in both electrodes.

The quantity $Y(\omega,\theta)$ is the barrier penetration factor [83,99,100] for quasiparticles with the energy ω that move in the direction comprising the angle θ with the junction normal. Note that, strictly speaking, for quasiparticles moving in the backward direction, the barrier transparency factor is $Y(\omega-eV,\theta)$ rather than $Y(\omega,\theta)$. Anyway, the actual tunnel barriers in break-junction experiments are rather high, so that the main contribution to the current is made by quasiparticles located in the vicinity of the Fermi level. Moreover, relevant voltages are of the order $V \le \Delta(T,\theta)/e$. Hence, we may put $Y(\omega-eV,\theta)$ to be energy-independent, so that

$$Y(\omega-eV,\theta) \approx Y(\omega,\theta) \to AY(\theta), \tag{4}$$

where the coefficient A is identical for all relevant ω. As a result, the factor A, as well as the electron densities of states N_F and N'_F, can be factorized out of the integrals to form, together with other pre-integral multipliers, the junction resistance in the normal state, R. The standard factor $\cos\theta$ makes allowance only for the normal projection of the quasiparticle motion with respect to the tunnel junction plane while calculating the total tunnel current through the junction [100–102]. This factor, together with the function $Y(\theta)$ [formula (4)], makes the contribution of a tunneling quasiparticle into the total current dependent on the angle at which the quasiparticle transverses the junction. This is the so-called tunnel directionality [55,82–86,103].

The importance of the tunnel directionality, which was recognized long ago, can strongly manifest itself when interpreting the quasiparticle currents across the break-junctions. Indeed, the voltage dependences of tunnel conductance $G(V)$, i.e. the differential quasiparticle current-voltage characteristics, for symmetric junctions are routinely used to determine the superconducting energy gap in the junction electrodes. Namely, the energy distance between the gap edges (the peak-to-peak separation) is assumed equal to 4Δ [73,104–106]. However, the phenomenon of tunnel directionality for a break junction fabricated from a *d*-wave superconductor may mislead the observer. Namely, for certain electrode configurations, it can effectively "cut off" the contribution of those Fermi surface sections that fall outside the "tunneling cone" ($|\theta| > \theta_0$, see Fig. 2), so that the corresponding gap values will not affect the actual CVCs. The consequences are considered below in more detail. To make them more illustrative, in this paper, we analyzed the following parabolic barrier-penetration function:

$$Y(\theta') \sim \begin{cases} \theta_0^2 - \theta^2 \text{ if } |\theta| \le \theta_0, \\ 0 \qquad \text{overwise}. \end{cases} \tag{5}$$

The selected phenomenological model totally excludes the participation of the Fermi surface sections falling outside the tunneling cone θ_0 in the CVC formation. It was done intentionally in order to make the directionality effect more dramatic and bearing in mind that, unfortunately, one cannot select the most adequate $Y(\theta)$ dependence on the basis of experiment. Nevertheless, the very existence and the character of the tunnel directionality (see, e.g., Refs. 55, 82–86) are satisfactorily described by the simple phenomenological function (5).

Furthermore, it is clear that, in the framework of the model concerned, the effectiveness of certain Fermi surface sections in the CVC formation strongly depends on the orientation of the break-junction electrode crystal lattices relative to the junction plane. This orientation will be described by the angle γ for the 0-electrode and γ' for the V-one; the both being reckoned from the junction normal to the corresponding superconducting lobe bisectrix. Since we consider symmetric junctions between two identical *d*-wave BCS superconductors, the common superconducting order parameter amplitude Δ_0 can be chosen as the energy scale and used to present the results in the normalized dimensionless form. As a result, the angular characteristics θ_0, γ, and γ' (together with the temperature T) are the only parameters of the problem.

Taking all the aforesaid into account, formula (1) can be rewritten in the form

$$J(V) = \frac{1}{4\pi R}\int\limits_{-\pi/2}^{\pi/2} d\theta \cos\theta\, Y(\theta) \times \\ \times \int\limits_{-\infty}^{\infty} d\omega\, K(\omega,V,T) P(\omega,\theta) P'(\omega-eV,\theta), \tag{6}$$

where

$$P(\omega,\theta) = \frac{|\omega|\,\Theta\left(|\omega| - \Delta(T,\theta)\right)}{\sqrt{\omega^2 - \Delta^2(T,\theta)}}, \tag{7}$$

and $\Theta(\omega)$ is the Heaviside unit step function. If the barrier-transparency function is normalized to unity,

$$\int\limits_{-\pi/2}^{\pi/2} d\theta\, Y(\theta) = 1, \tag{8}$$

the pre-integral coefficient ensures the correct (Ohmic) current asymptotics at large $|V|$'s:

$$\lim_{V\to\pm\infty} J(V) = \frac{V}{R}. \tag{9}$$

One should pay attention that the quantity

$$\frac{1}{R}\int\limits_{-\infty}^{\infty} d\omega\, K(\omega,V,T) P(\omega,\theta) P'(\omega-eV,\theta) \tag{10}$$

in Eq. (6) is proportional to the tunnel current through a symmetric junction between two *s*-wave superconductors [45]. Hence, formula (6) can be interpreted as the coherent averaging of quasiparticle current in the momentum space (over the angle θ) with the weight $\cos\theta\, Y(\theta)$.

It is known [46–48] that the voltage dependence of the tunnel conductance $G = dJ/dV$, i.e. $G(V)$, is much more informative than the voltage dependence of the tunnel current itself, i.e. $J(V)$. By making trivial transformations, the dependence $G(V)$ can be reduced to the dimensionless form $g(v)$, with $g = RG$ and $v = eV/\Delta_0$. So, the dependences $g(v)$ were calculated by simulating the experimental routine. In particular, a formula that can be reduced to the expression

$$g(v) = R\frac{J(V+\delta V) - J(V-\delta V)}{2\delta V}, \qquad (11)$$

in which the current J was calculated numerically, since analytical integration was impossible even in the case $T = 0$. (For a more detail discussion of this issue, see, e.g., Ref. 107.) The increment δv of the dimensionless bias voltage for the numerical differentiation of the dependence $J(V)$ was selected to equal $\delta v = e\delta V/\Delta_0 = 0.001$.

3. Results of calculation and discussion

The general arrangement of the rotated *d*-wave (or extended *s*-wave) superconducting electrodes on the both sides of the break junction is shown in Fig. 2. In this work dealing with the combined effect of tunnel directionality and the anisotropy of the superconducting gap in *d*-wave (extended *s*-wave) superconductors on the quasiparticle current, we confined the analysis to the cases when either or both electrodes are oriented at an angle of 0° or 45° with respect to the junction normal **n**. The both orientations are shown in Fig. 2. The figure also demonstrates the "tunnel cones" $2\theta_0$, which "give" a contribution to the tunnel current. From the figure, one can easily get an idea how the rotation of electrodes engages the FS sections that effectively participate in quasiparticle tunneling.

The conductances $G(V)$ for the symmetric S–I–S junction obtained by cracking a single piece of *d*-wave superconductor without any rotations in the *ab* plane ($\gamma = \gamma' = 0^\circ$) are shown in Fig. 3 for explicitly indicated tunneling cone parameters θ_0 and various reduced temperatures T/T_c. Here, $T_c = \frac{\gamma_E\sqrt{e}}{2\pi}\Delta_0$ is the critical temperature for the

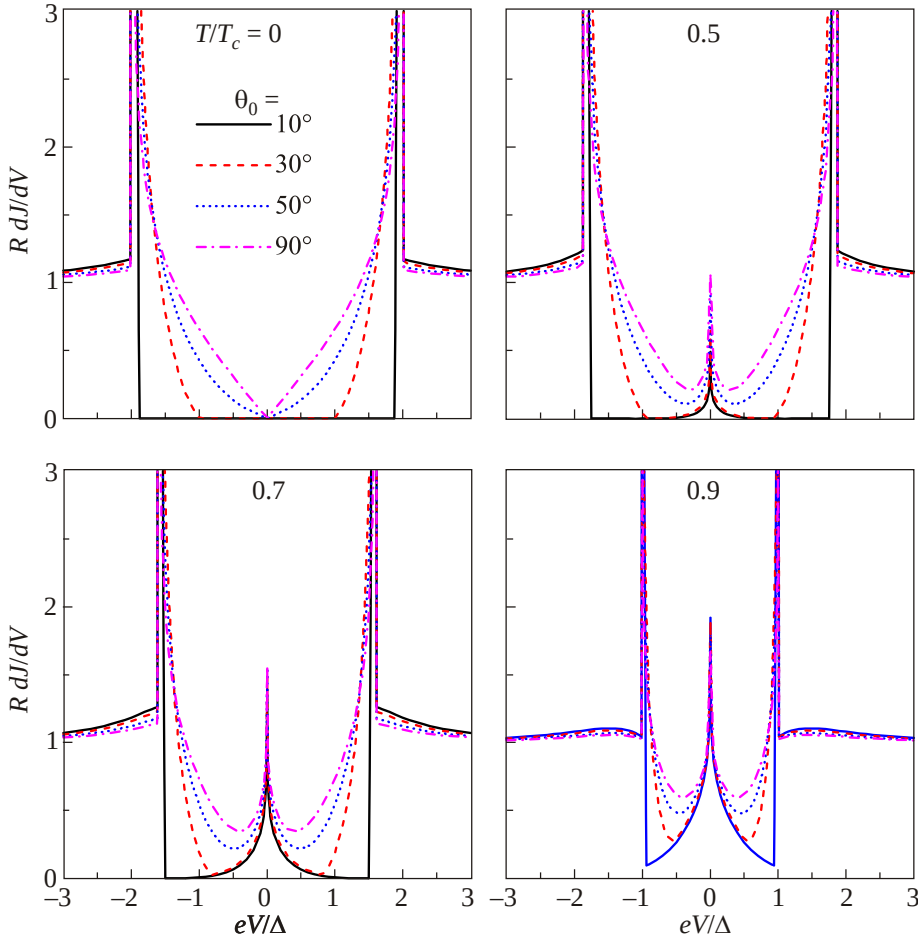

Fig. 3. (Color online) CVCs for break junctions with various θ_0's and at various T/T_c's. The electrode orientations are $\gamma = \gamma' = 0^\circ$.

$d_{x^2-y^2}$-wave (extended *s*-wave) superconductor, $\gamma_E \approx 0.5771$ is the Euler constant, and e ≈ 2.718 is the base of natural logarithms. One sees that at $T/T_c = 0$, the CVC behavior near $V = 0$ varies from the *s*-wave-like [47] (for small θ_0's) to the *d*-wave-like (for large θ_0's) one [49]. However, the overall behavior and especially the form of $G(V)$ near the gap edges conspicuously differ from the curves for S–I–S junctions [49] depicted in Fig. 1 even for thin interlayers (at large θ_0's). It is no wonder, because the directionality effects were not taken into account in Ref. 49.

Specifically, the authors of Ref. 49 calculated $G(V)$ both for S–I–S and S–I–N junctions by means of separate angular (over θ and θ′) averaging of the gapped electron densities of states (2) for each electrode and subsequent integration over the energy variable ω (in our notations). Therefore, only one angular integration was performed while calculating $G(V)$ for S–I–N junctions and two integrations in the case of the S–I–S ones. In essence, this procedure is the realization of the incoherent tunneling regime. Moreover, the "directionality factors" $\cos\theta$ and $Y(\theta)$ were omitted from consideration, which allowed the cited authors to obtain analytical expressions. (One should pay attention that the interpretation of the angle θ, at which a quasiparticle crosses the barrier, faces difficulties in the case of incoherent tunneling.) On the contrary, we take the directionality into account, so that the both "directionality factors" enter the consideration. Hence, we integrate over the single angle θ, which is the feature appropriate to the coherent tunneling. That is why our CVCs for S–I–S junctions are similar to those for S–I–N junctions found in Ref. 49.

All the aforesaid means that the uncontrollable directionality determines the apparent form of $G(V)$ and makes CVCs neither truly *d*-wave nor *s*-wave ones. As a consequence, the tunnel break junction CVC measurements cannot serve as an unambiguous evidence of the superconducting order parameter symmetry, contrary to what is frequently argued. Thus, discrepancies between the results obtained even for break junctions produced from cuprate samples taken from the same batch can be interpreted as caused by different directionality cones θ_0's, which can be associated, e.g., with *different interelectrode distances*. The same phenomena might have already been observed in break-junction experiments with other layered materials demonstrating a controversy about the order parameter symmetry, e.g., iron-based superconductors [108,109].

For finite temperatures, the gap amplitude is reduced in a usual way and decreases the distance between the gap-related maxima in $G(V)$. A new feature, which appears at $V = 0$ and finite T's, is proportional to $\ln V$ and rapidly grows with T. This zero-bias peak is well-known for isotropic *s*-wave superconductors and reflects the rise of conductance resulting from the thermal filling of quasiparticle states primarily just below and above the energy gaps in both electrodes. The effect is especially strong when the upper and lower gap edges almost coincide ($V \to 0$) [44]. Such a behavior persists for the configuration concerned, although the order parameters are not constant but proportional to $\cos 2\theta$ for the anisotropic superconductivity. The low-V peculiarity should be observed in *d*-wave break junctions, mimicking the isotropic pairing picture. Note that this peculiarity is much more pronounced than that predicted in the Won–Maki model [49,50] (see Fig. 1(b)).

It is well-known that, in principle, the electrode surfaces in break junctions are not atomically smooth. Instead, they are usually very rough. As a result, the junction interlayer can be oriented (this orientation is determined by the orientation of the vector **n** normal to both electrodes, see Fig. 2) at an angle $-\gamma \neq 0°$ with respect to the $\mathbf{k}_x$ axis. This configuration can be interpreted as both electrodes simultaneously rotated by the angle γ with respect to the junction plane. For simplicity, we consider the limiting configuration: a symmetric junction with $\gamma = \gamma' = 45°$. The corresponding $G(V)$ is shown in Fig. 4. In such a junction, whatever the directionality cone θ_0, the conductance $G(V)$ has the V-form near the bias-voltage origin, thus being apparently a *d*-wave like from this point of view. At the same time, for large interelectrode distances (small θ_0's), the peak-to-peak separation is much smaller than that estimated from the independently measured superconducting-gap amplitude Δ_0. Furthermore, the peaks are smeared and low. Only for extremely large θ_0's, the patterns looking like the "textbook" *d*-wave CVCs (see Fig. 1) are reproduced with an accuracy of the angular integration peculiarities (see the discussion above). At finite temperatures ($T \neq 0$), the peak-to-peak separation is reduced and the logarithmic peak appears in the vicinity of $V = 0$, being quite similar to its counterpart in the configuration $\gamma = \gamma' = 0°$ (Fig. 3).

One can see, that the CVCs obtained in both considered cases ($\gamma = \gamma' = 0°$ and $\gamma = \gamma' = 45°$) are rather different. In addition, owing to the break-junction gap roughness, the interelectrode gap in the "active" junction section can be oriented at an arbitrary angle $-\gamma$ within the interval 0–45° (those angles are not considered here). Furthermore, if we adopt that quasiparticle tunneling can take place at several points over the interelectrode gap with different values of the normal vector **n**, we must be ready to approximate experimental CVCs by a linear sum of theoretical CVCs corresponding to different **n** orientations and taken with unknown weights (different R values). Therefore, one can hardly find such a set of break-junction measurements that can be directly compared to CVCs for configurations $\gamma = \gamma' = 0°$ and $\gamma = \gamma' = 45°$. However, experiments, very similar to the break-junction ones, were made to study tunneling between thin crystals of $Bi_2Sr_2CaCu_2O_{8+\delta}$ in a crossing configuration [110]. Those measurements showed that the peak-to-peak separation was approximately twice as much for $\gamma = \gamma' = 0°$ than for $\gamma = \gamma' = 45°$. The observations agree with our (purely *d*-wave!) calculations with

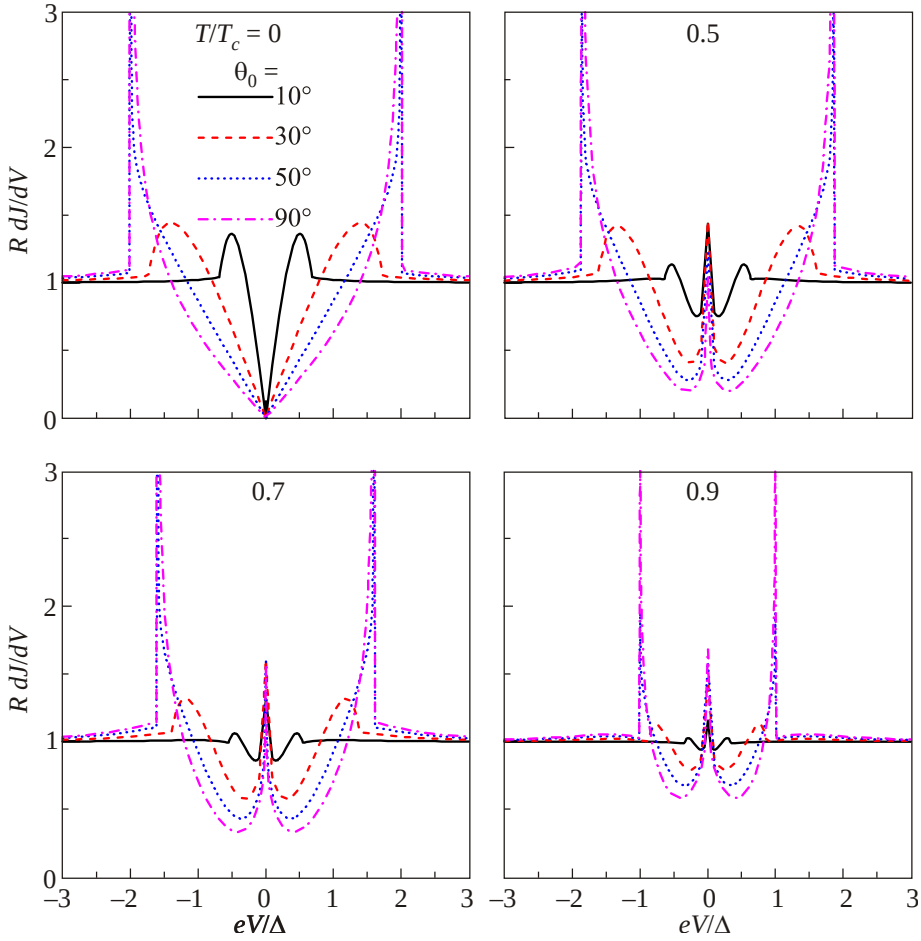

Fig. 4. (Color online) The same as in Fig. 3, but for $\gamma = \gamma' = 45^\circ$.

quite a reasonable $\theta_0 \approx 30°$. Nevertheless, the forms of the CVCs differ substantially from the theoretical curves. Thus, it is impossible to consider those experiments as a reliable confirmation of the *d*-wave order parameter symmetry in $Bi_2Sr_2CaCu_2O_{8+\delta}$, although the inferred energy gap is undoubtedly anisotropic.

Finally, let us consider a possible symmetric S–I–S configuration with $\gamma = 45°$ and $\gamma' = 0°$. It is of special interest, since in this case the apparent *s*- and *d*-like features of both pieces interfere in the resulting CVCs. The results of calculation are demonstrated in Fig. 5. One can readily see that, at $T/T_c = 0$, the conductance curves $G(V)$ are more or less of the *s*-type for all directionality cones. At small cones, $\theta_0 \leq 10°$, one more interesting property is observed. Namely, the gap-related peaks are located at $V \approx \pm\Delta_0/e$ rather than at $V \approx \pm 2\Delta_0/e$, as it should be for S–I–S configurations. Hence, the CVCs look like those inherent to S_i–I–N junctions made of *s*-wave superconductors. For larger θ_0's up to $\theta_0 = 90°$, the $G(V)$ dependences are distorted, so that there are deviations of gap edges towards larger V, although the locations $\pm 2\Delta_0/e$, which are characteristic of S–I–S junctions, are never achieved. Such apparent S_i–I–N conductance-voltage characteristics were observed, e.g., in nominally S–I–S junctions with $YBa_2Cu_3O_{7-\delta}$ [111] and $La_{1.85}Sr_{0.15}CuO_4$ [112] electrodes.

Thermal effects in the ($\gamma = 45°$, $\gamma' = 0°$) configuration are very peculiar. First of all, the CVCs at $T \neq 0$ include conspicuous negative blowouts in the gap region. Negative portions of $G(V)$ are not forbidden by any general consideration [107], still being somewhat exotic. They were observed, e.g., in $Bi_2Sr_2CaCu_2O_{8+\delta}$ break junctions [113]. Their origin was attributed either to CDWs [107] or resonance spin excitations [113], the both assumptions seeming quite plausible. In our theory, any complications of this type are absent, so that the effect of negative $G(V)$ is caused by the difficulty of tunneling between thermally filled states above and below the gap edges, when the quasiparticles tunnel from the node of one electrode into the antinode FS region of the other one. One should expect that any disorder effects will substantially smear the negative spikes.

Heating also leads to the appearance of sub-gap structures in the ($\gamma = 45°$, $\gamma' = 0°$) junctions (Fig. 5). They, however, differ significantly from their counterparts in the $\gamma = \gamma' = 0°$ and $\gamma = \gamma' = 45°$ junctions (Figs. 3 and 4, respectively). Specifically, for large θ_0's, a broad maximum develops near $V = 0$ and replaces the sharp logarithmic singularity intrinsic to $\gamma = \gamma'$ configurations (Figs. 3 and 4). This phenomenon is associated with the superposition of contributions from different segments of the FSs in the left (0-)

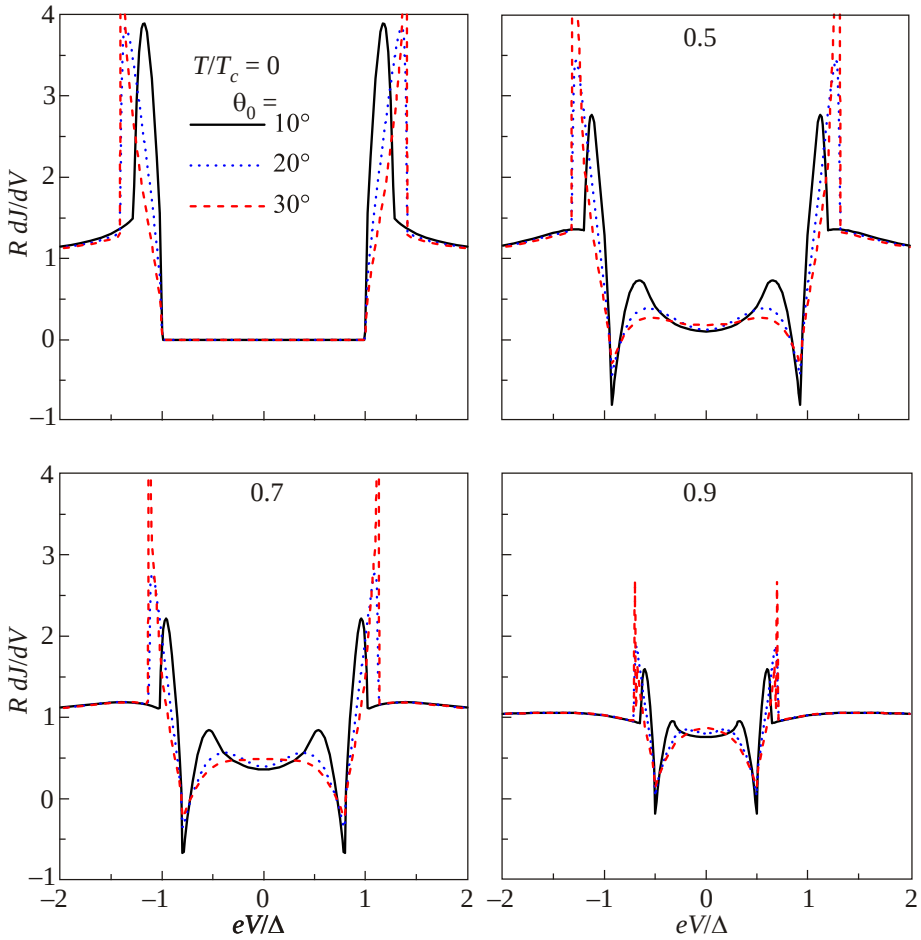

Fig. 5. (Color online) The same as in Fig. 3, but for $\gamma = 45^\circ$ and $\gamma' = 0^\circ$. All plots with $\theta_0 > 30^\circ$ are very similar to the corresponding plots with $\theta_0 = 30^\circ$ and therefore are not included.

and right (V-) electrodes. The picture changes drastically for smaller θ_0's. Then, the logarithmic singularity is restored, but it corresponds now to the *difference* between the finite temperature-dependent gap value at $\gamma' = 0°$ to the right and a negligibly small gap at $\gamma = 45°$ to the left of the junction. Such a property is well known for isotropic *s*-wave superconductors [114]. The pair of maxima at finite V values, which appear when $T \neq 0$, become more pronounced for decreasing θ_0, but they are never as sharp as the logarithmic singularities near $V = 0$ emerging in the $\gamma = \gamma' = 0°$ and $\gamma = \gamma' = 45°$ junctions.

For other rotations of crystal lattices with respect to the break-junction plane, the CVC patterns become more complex and involve features appropriate to their symmetric counterparts. The sub-gap features that arise due to different relative electrode orientations deserve to be sought in the measurement results obtained for both cuprates and other layered superconductors, which are suspected to possess the *d*-wave order parameter symmetry (for instance, the attribution of peculiarities in intrinsic mesa junctions made of $Bi_2Sr_2CaCu_2O_{8+\delta}$ [56] may be revised). The actual $G(V)$ are of course even more intricate, because additional pseudogap (i.e. CDW) contributions appear in many of such materials [26,55,60,73,76–78,107,115–118].

To trace the evolution of CVCs with the interelectrode distance and rotation angles in detail, it would be useful to complement break-junction measurements by other experiments with angle-resolved electron tunneling between layered *d*-wave superconductors. In particular, the crossing tunneling [110] may be used, or ring ramp-edge high-T_c oxide samples [10,32,119] should be harnessed with the counter-electrode also made of the same high-T_c oxide. Then, one should be able to controllably change the junction configurations with small steps in γ and γ'.

4. Conclusions

Our study of the tunneling in the *ab* plane in break junctions composed of layered *d*-wave superconductors demonstrated a strong dependence of the corresponding CVCs on the directionality cone $2\theta_0$ width, i.e. on the interlayer distance, and the rotation angles γ and γ' of the electrode crystal lattices with respect to the junction plane. It was shown that, although the intrinsic Cooper pairing symmetry in the electrode material is the *d*-wave one, the conductances $G(V)$ may exhibit predominantly *d*-wave, *s*-wave or mixed forms, depending on θ_0, which in its turn may be changed by adjusting the interelectrode

distance. Moreover, the CVCs for essentially S–I–S junctions may acquire forms similar to those appropriate to the S–I–N junctions if the angular configuration involves 45° and $\gamma' = 0°$. For finite temperatures, the sub-gap features demonstrate peculiar forms reflecting the spread of the electrode energy gap values and the absence of matching between the left and right gap amplitudes. Our calculations can be applied not only to break junctions, but also to other experimental setups, for instance, to those used to study the Josephson currents flowing in the *ab* plane of specially prepared cuprate structures [10,32,110,119]. The results obtained above were discussed with an emphasis on high-T_c oxides. However, the adopted basic model is common to any *d*-wave layered superconductors and layered superconductors with the hypothetical extended *s*-wave symmetry of their order parameter.

Acknowledgments

The work was partially supported by the Project No 24 of the 2015–2017 Scientific Cooperation Agreement between Poland and Ukraine.

1. J.G. Bednorz and K.A. Müller, *Z. Phys. B* **64**, 189 (1986).
2. H.-U. Habermeier, *Fiz. Nizk. Temp*. **42**, 1075 (2016) [*Low Temp. Phys*. **42**, 840 (2016)].
3. T. Moriya and K. Ueda, *Adv. Phys*. **49**, 555 (2000).
4. A.A. Kordyuk and S.V. Borisenko, *Fiz. Nizk. Temp*. **32**, 401 (2006) [*Low Temp. Phys*. **32**, 298 (2006)].
5. A.-M.S. Tremblay, B. Kyung, and D. Sénéchal, *Fiz. Nizk. Temp*. **32**, 561 (2006) [*Low Temp. Phys*. **32**, 424 (2006)].
6. E.G. Maksimov and O.V. Dolgov, *Usp. Fiz. Nauk* **177**, 983 (2007).
7. J.P. Carbotte, T. Timusk, and J. Hwang, *Rep. Prog. Phys*. **74**, 066501 (2011).
8. C.M. Varma, *Rep. Prog. Phys*. **75**, 052501 (2012).
9. R.A. Klemm, *Philos. Mag*. **85**, 801 (2005).
10. J.R. Kirtley, *C.R. Physique* **12**, 436 (2011).
11. V.P. Mineev and K.V. Samokhin, *Intoduction into the Theory of Non-Conventional Superconductors*, MFTI Publishing House, Moscow (1998), in Russian.
12. M.L. Kulić, *Phys. Rep*. **338**, 1 (2000).
13. A.S. Alexandrov, *Phys. Scr*. **83**, 038301 (2011).
14. J.C. Phillips, *Proc. Nat. Acad. Sci. USA* **107**, 1307 (2010).
15. J. Bardeen, L.N. Cooper, and J.R. Schrieffer, *Phys. Rev*. **108**, 1175 (1957).
16. A.M. Gabovich and V.I. Kuznetsov, *Eur. J. Phys*. **34**, 371 (2013).
17. J.P. Carbotte, *Rev. Mod. Phys*. **62**, 1027 (1990).
18. A.A. Varlamov, G. Balestrino, E. Milani, and D.V. Livanov, *Adv. Phys*. **48**, 655 (1999).
19. A. Damascelli, Z. Hussain, and Z.-X. Shen, *Rev. Mod. Phys*. **75**, 473 (2003).
20. D. Manske, *Theory of Unconventional Superconductors. Cooper-Pairing Mediated by Spin Excitations*, Springer Verlag, New York (2004).
21. M. Eschrig, *Adv. Phys*. **55**, 47 (2006).
22. N.E. Hussey, *J. Phys.: Condens. Matter* **20**, 123201 (2008).
23. N.P. Armitage, P. Fournier, and R.L. Greene, *Rev. Mod. Phys*. **82**, 2421 (2010).
24. A.A. Kordyuk, V.B. Zabolotnyy, D.V. Evtushinsky, D.S. Inosov, T.K. Kim, B. Büchner, and S.V. Borisenko, *Eur. Phys. J. Special Topics* **188**, 153 (2010).
25. N.M. Plakida, *High-Temperature Cuprate Superconductors. Experiment, Theory, and Applications*, Springer Verlag, Berlin (2010).
26. A.A. Kordyuk, *Fiz. Nizk. Temp*. **41**, 417 (2015) [*Low Temp. Phys*. **41**, 319 (2015)].
27. G.G. Sergeeva, Yu.P. Stepanovskii, and A.V. Chechkin, *Fiz. Nizk. Temp*. **24**, 1029 (1998) [*Low Temp. Phys*. **24**, 771 (1998)].
28. C.C. Tsuei and J.R. Kirtley, *Rev. Mod. Phys*. **72**, 969 (2000).
29. H.J.H. Smilde, A. Ariando, D.H.A. Blank, G.J. Gerritsma, H. Hilgenkamp, and H. Rogalla, *Phys. Rev. Lett*. **88**, 057004 (2002).
30. H. Hilgenkamp and J. Mannhart, *Rev. Mod. Phys*. **74**, 485 (2002).
31. Yu.A. Kolesnichenko, A.N. Omelyanchouk, and A.M. Zagoskin, *Fiz. Nizk. Temp*. **30**, 714 (2004) [*Low Temp. Phys*. **30**, 535 (2004)].
32. J.R. Kirtley, C.C. Tsuei, A. Ariando, C.J.M. Verwijs, S. Harkema, and H. Hilgenkamp, *Nature Phys*. **2**, 190 (2006).
33. C.C. Tsuei and J.R. Kirtley, in: *Superconductivity. Vol. 2: Novel Superconductors*, K.H. Bennemann and J.B. Ketterson (eds.), Springer Verlag, Berlin (2008), p. 869.
34. H. Hilgenkamp, *Supercond. Sci. Technol*. **21**, 034011 (2008).
35. H. Kimura, R.P. Barber, Jr, S. Ono, Y. Ando, and R.C. Dynes, *Phys. Rev. B* **80**, 144506 (2009).
36. A.S. Katz, A.G. Sun, and R.C. Dynes, *Appl. Phys. Lett*. **66**, 105 (1995).
37. R. Kleiner, A.S. Katz, A.G. Sun, R. Summer, D.A. Gajewski, S.H. Han, S.I. Woods, E. Dantsker, B. Chen, K. Char, M.B. Maple, R.C. Dynes, and J. Clarke, *Phys. Rev. Lett*. **76**, 2161 (1996).
38. K.A. Kouznetsov, A.G. Sun, B. Chen, A.S. Katz, S.R. Bahcall, J. Clarke, R.C. Dynes, D.A. Gajewski, S.H. Han, M.B. Maple, J. Giapintzakis, J.-T. Kim, and D.M. Ginsberg, *Phys. Rev. Lett*. **79**, 3050 (1997).
39. Q. Li, Y.N. Tsay, M. Suenaga, R. A. Klemm, G.D. Gu, and N. Koshizuka, *Phys. Rev. Lett*. **83**, 4160 (1999).
40. Yu.I. Latyshev, A.P. Orlov, A.M. Nikitina, P. Monceau, and R.A. Klemm, *Phys. Rev. B* **70**, 094517 (2004).
41. H. Kimura, R.P. Barber, Jr, S. Ono, Y. Ando, and R.C. Dynes, *Phys. Rev. Lett*. **101**, 037002 (2008).
42. R.A. Klemm, *Layered Superconductors*, Vol. 1, University Press, Oxford (2012).
43. D.H. Douglass, Jr, and L.M. Falicov, *Progr. Low Temp. Phys*. **4**, 97 (1964).
44. A.I. Larkin and Yu.N. Ovchinnikov, *Zh. Éksp. Teor. Fiz*. **51**, 1535 (1966) [*Sov. Phys. JETP* **24**, 1035 (1966)].
45. A. Barone and G. Paterno, *The Physics and Applications of the Josephson Effect*, John Wiley and Sons, New York (1982).
46. I. Giaever, *Phys. Rev. Lett*. 5, 147 (1960).

47. I. Giaever, *Phys. Rev. Lett*. **5**, 464 (1960).
48. I. Giaever and K. Megerle, *Phys. Rev*. **122**, 1101 (1961).
49. H. Won and K. Maki, *Phys. Rev. B* **49**, 1397 (1994).
50. H. Won, Y. Morita, and K. Maki, *Phys. Status Solidi B* **244**, 4371 (2007).
51. X.-H. Sui, H.-T. Wang, H. Tang, and Z.-B. Su, *Phys. Rev. B* **94**, 144505 (2016).
52. A. Yurgens, D. Winkler, T. Claeson, S.-J. Hwang, and J.-H. Choy, *Int. J. Mod. Phys. B* **13**, 3758 (1999).
53. A.A. Yurgens, V.M. Krasnov, D. Winkler, and T. Claeson, *Curr. Appl. Phys*. **1**, 413 (2001).
54. G.A. Ovsyannikov and K.Y. Constantinian, *Fiz. Nizk. Temp*. **38**, 423 (2012) [*Low Temp. Phys*. **38**, 333 (2012)].
55. V.M. Krasnov, *Phys. Rev. B* **91**, 224508 (2015).
56. V.M. Krasnov, *Phys. Rev. B* **93**, 064518 (2016).
57. Th. Jacobs, S.O. Katterwe, and V.M. Krasnov, *Phys. Rev. B* **94**, 220501 (2016).
58. A. M. Gabovich and A. I. Voitenko, *Physica C* **503**, 7 (2014).
59. A.M. Gabovich, M.S. Li, H. Szymczak, and A.I. Voitenko, *Phys. Rev. B* **92**, 054512 (2015).
60. A.M. Gabovich and A.I. Voitenko, *Fiz. Nizk. Temp*. **42**, 1103 (2016) [*Low Temp. Phys*. **42**, 863 (2016)].
61. T. Ekino, A.M. Gabovich, M.S. Li, H. Szymczak, and A.I. Voitenko, *J. Phys.: Condens. Matter* **28**, 445701 (2016).
62. J. Moreland and J.W. Ekin, *J. Appl. Phys*. **58**, 5888 (1985).
63. J.R. Kirtley, *Int. J. Mod. Phys. B* **4**, 201 (1990).
64. T. Ekino, T. Takabatake, H. Tanaka, and H. Fujii, *Phys. Rev. Lett*. **75**, 4262 (1995)
65. T. Ekino, T. Doukan, and H. Fujii, *J. Low Temp. Phys*. **105**, 563 (1996).
66. R.J.P. Keijsers, O.I. Shklyarevskii, J.G.H. Hermsen, and H. van Kempen, *Rev. Sci. Instrum*. **67**, 2863 (1996).
67. T. Ekino, T. Takasaki, T. Muranaka, J. Akimitsu, and H. Fujii, *Phys. Rev. B* **67**, 094504 (2003).
68. T.E. Shanygina, Ya.G. Ponomarev, S.A. Kuzmichev, M.G. Mikheev, S.N. Tchesnokov, O.E. Omel'yanovskii, A.V. Sadakov, Yu.F. Eltsev, A.S. Dormidontov, V.M. Pudalov, A. Usol'tsev, and E.P. Khlybov, *Pis'ma Zh. Éksp. Teor. Fiz*. **93**, 95 (2011).
69. T. Ekino, A. Sugimoto, Y. Sakai, A.M. Gabovich, and J. Akimitsu, *Fiz. Nizk. Temp*. **40**, 1182 (2014) [*Low Temp. Phys*. **40**, 925 (2014)].
70. S.A. Kuzmichev and T.E. Kuzmicheva, *Fiz. Nizk. Temp*. **42**, 1284 (2016) [*Low Temp. Phys*. **42**, 1008 (2016)].
71. D. Mandrus, J. Hartge, C. Kendziora, L. Mihaly, and L. Forro, *Europhys. Lett*. **22**, 199 (1993).
72. Ya.G. Ponomarev, B.A. Aminov, M.A. Hein, H. Heinrichs, V.Z. Kresin, G. Müller, H. Piel, K. Rosner, S.V. Tchesnokov, E.B. Tsokur, D. Wehler, R. Winzer, A.V. Yarygin, and K.T. Yusupov, *Physica C* **243**, 167 (1995).
73. T. Ekino, Y. Sezaki, and H. Fujii, *Phys. Rev. B* **60**, 6916 (1999).
74. S.I. Vedeneev and D.K. Maude, *Phys. Rev. B* **72**, 144519 (2005).
75. J. Hartge, L. Forr, D. Mandrus, M.C. Martin, C. Kendziora, and L. Mihaly, *J. Phys. Chem. Sol*. **54**, 1359 (1993).
76. A.M. Gabovich and A.I. Voitenko, *Fiz. Nizk. Temp*. **26**, 419 (2000) [*Low Temp. Phys*. **26**, 305 (2000)].
77. A.M. Gabovich, A.I. Voitenko, T. Ekino, M.S. Li, H. Szymczak, and M. Pékała, *Adv. Condens. Matter Phys*. 2010, Article ID 681070 (2010).
78. A.M. Gabovich and A.I. Voitenko, *Fiz. Nizk. Temp*. **39**, 301 (2013) [*Low Temp. Phys*. **39**, 232 (2013)].
79. F. Tafuri and J.R. Kirtley, *Rep. Prog. Phys*. **68**, 2573 (2005).
80. J.R. Kirtley and F. Tafuri, in: *Handbook of High-Temperature Superconductivity. Theory and Experiment*, J.R. Schrieffer and J.S. Brooks (eds.), Springer Verlag, New York (2007), p. 19.
81. F. Tafuri, D. Massarotti, L. Galletti, D. Stornaiuolo, D. Montemurro, L. Longobardi, P. Lucignano, G. Rotoli, G.P. Pepe, A. Tagliacozzo, and F. Lombardi, *J. Supercond.* **26**, 21 (2013).
82. I.O. Kulik and I.K. Yanson, *Josephson Effect in Superconducting Tunneling Structures*, Coronet, New York (1971).
83. E.L. Wolf, *Principles of Electron Tunneling Spectroscopy*, Oxford University Press, New York (1985).
84. M. Ledvij and R.A. Klemm, *Phys. Rev. B* **51**, 3269 (1995).
85. D. Daghero, M. Tortello, P. Pecchio, V.A. Stepanov, and R.S. Gonnelli, *Fiz. Nizk. Temp*. **39**, 261 (2013) [*Low Temp. Phys*. **39**, 199 (2013)].
86. A.M. Gabovich, M.S. Li, H. Szymczak, and A.I. Voitenko, *Phys. Rev. B* **87**, 104503 (2013).
87. J.F. Annett, *Adv. Phys*. **39**, 83 (1990).
88. J.F. Annett, *Contemp. Phys*. **36**, 423 (1995).
89. D. Koelle, R. Kleiner, F. Ludwig, E. Dantsker, and J. Clarke, *Rev. Mod. Phys*. **71**, 631 (1999).
90. S. Kashiwaya and Y. Tanaka, *Rep. Prog. Phys*. **63**, 1641 (2000).
91. D.J. Scalapino, *Rev. Mod. Phys*. **84**, 1383 (2012).
92. P.B. Littlewood, *Phys. Rev. B* **42**, 10075 (1990).
93. C.C. Tsuei and J.R. Kirtley, *Phys. Rev. Lett*. **85**, 182 (2000).
94. G-m. Zhao, *Phys. Rev. B* **64**, 024503 (2001).
95. B.H. Brandow, *Phys. Rev. B* **65**, 054503 (2002).
96. B.H. Brandow, *Philos. Mag*. **83**, 2487 (2003).
97. M. Ogata and H. Fukuyama, *Rep. Prog. Phys*. **71**, 036501 (2008).
98. M.H. Cohen, L.M. Falicov, and J.C. Phillips, *Phys. Rev. Lett*. **8**, 316 (1962).
99. J. Frenkel, *Phys. Rev*. **36**, 1604 (1930).
100. A. Sommerfeld and H. Bethe, *Elektronentheorie der Metalle*, Springer Verlag, Berlin (1933).
101. Yu.S. Barash, A.V. Galaktionov, and A.D. Zaikin, *Phys. Rev. Lett*. **75**, 1676 (1995).
102. A.M. Gabovich and A.I. Voitenko, *Fiz. Nizk. Temp*. **38**, 414 (2012) [*Low Temp. Phys*. **38**, 326 (2012)].
103. Y-m. Nie and L. Coffey, *Phys. Rev. B* **59**, 11982 (1999).
104. T. Ekino, H. Fujii, M. Kosugi, Y. Zenitani, and J. Akimitsu, *Phys. Rev. B* **53**, 5640 (1996).
105. A.I. D'yachenko, V.Yu. Tarenkov, R. Szymczak, H. Szymczak, A.V. Abal'oshev, S.J. Lewandowski, and L. Leonyuk, *Fiz. Nizk. Temp*. **29**, 149 (2003) [*Low Temp. Phys*. **29**, 108 (2003)].

106. T. Takasaki, T. Ekino, A. Sugimoto, K. Shohara, S. Yamanaka, and A.M. Gabovich, *Eur. Phys. J. B* **73**, 471 (2010).
107. T. Ekino, A.M. Gabovich, M.S. Li, M. Pékała, H. Szymczak, and A.I. Voitenko, *J. Phys.: Condens. Matter* **20**, 425218 (2008).
108. P. Seidel, *Supercond. Sci. Technol*. **24**, 043001 (2011).
109. M.R. Eskildsen, E.M. Forgan, and H. Kawano-Furukawa, *Rep. Prog. Phys*. **74**, 124504 (2011).
110. J. Kane and K.-W. Ng, *Phys. Rev. B* **53**, 2819 (1996).
111. T. Ekino, T. Minami, H. Fujii, and J. Akimitsu, *Physica C* **235–240**, 1899 (1994).
112. T. Ekino, T. Doukan, H. Fujii, F. Nakamura, S. Sakita, M. Kodama, and T. Fujita, *Physica C* **263**, 249 (1996).
113. J.F. Zasadzinski, L. Ozyuzer, N. Miyakawa, K.E. Gray, D.G. Hinks, and C. Kendziora, *Phys. Rev. Lett*. **87**, 067005 (2001).
114. S. Shapiro, P.H. Smith, J. Nicol, J.L. Miles, and P.F. Strong, *IBM J. Res. Dev*. **6**, 34 (1962).
115. T. Ekino, A.M. Gabovich, and A.I. Voitenko, *Fiz. Nizk. Temp*. **34**, 515 (2008) [*Low Temp. Phys*. **34**, 409 (2008)].
116. S.V. Borisenko, A.A. Kordyuk, A.N. Yaresko, V.B. Zabolotnyy, D.S. Inosov, R. Schuster, B. Büchner, R. Weber, R. Follath, L. Patthey, and H. Berger, *Phys. Rev. Lett*. **100**, 196402 (2008).
117. P. Monceau, *Adv. Phys*. **61**, 325 (2012).
118. A.A. Kordyuk, *Fiz. Nizk. Temp*. **40**, 375 (2014) [*Low Temp. Phys*. **40**, 286 (2014)].
119. H.J.H. Smilde, A.A. Golubov, Ariando, G. Rijnders, J.M. Dekkers, S. Harkema, D.H.A. Blank, H. Rogalla, and H. Hilgenkamp, *Phys. Rev. Lett*. **95**, 257001 (2005).